Macromolecules

Article

pubs.acs.org/Macromolecules

Preservation of Photoluminescence Efficiency in the Ordered phases of Poly(2,3-diphenyl-1,4-phenylenevinylene) via Disturbing the Intermolecular $\pi-\pi$ Interactions with Dendritic Aliphatic Side Chains

Yu-Chun Wu,[†] Xiang-Kui Ren,[‡] Er-Qiang Chen,[‡] Hsun-Mei Lee,[†] Jean-Luc Duvail,[§] Chien-Lung Wang,*[,†] and Chain-Shu Hsu*[,†]

[†]Department of Applied Chemistry, National Chiao Tung University, 1001 Ta Hsueh Road, Hsin-Chu 30010, Taiwan

[‡]Beijing National Laboratory for Molecular Sciences, Department of Polymer Science and Engineering and Key Laboratory of Polymer Chemistry and Physics of Ministry of Education, College of Chemistry, Peking University, Beijing 100871, China

[§]Institut des Matériaux Jean Rouxel, UMR6502 CNRS, University of Nantes, F-44322 Nantes, France

Supporting Information

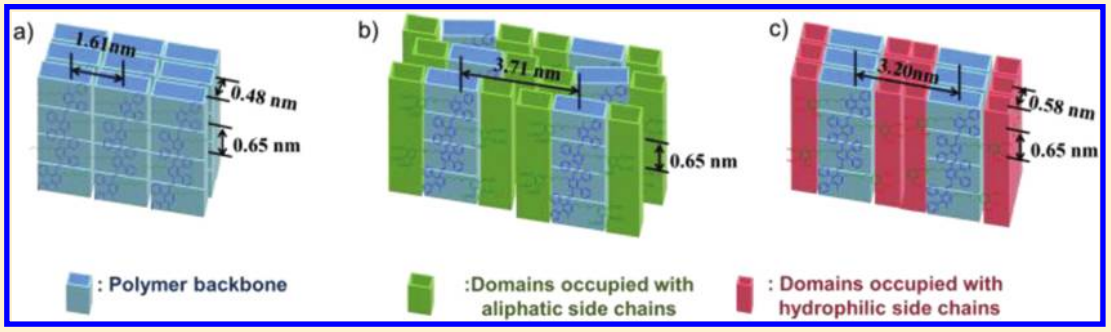

ABSTRACT: To understand the relation between the solid-state phase structures and the photophysical properties of poly(2,3-diphenyl-1,4-phenylenevinylene) (DP-PPV) derivatives, three DP-PPV derivatives, **P1**−**P3**, were designed, synthesized via Gilch polymerization and characterized. Among the polymers, **P1** is a reported highly emissive poly(2,3-diphenyl-5-hexyl-*p*-phenylenevinylene), and **P2** and **P3** are novel DP-PPV derivatives, which are purposely designed to bear hydrophobic and hydrophilic Percec-type dendrons as side chains. The bulkiness and hydrophobic−hydrophilic natures of the side chains show strong effects on photophysical properties of the polymers. The solutions and as-casted films of **P1**−**P3** all show remarkably high photoluminescence (PL) efficiency (Φ_{PL}) (>80% in chloroform solution, and >63% for the as-casted films). However, Φ_{PL} of **P1** and **P3** decrease significantly to 30% after cooled their polymer melts to room temperature. Through the phase behavior analysis by differential scanning calorimetry (DSC), and phase structure analysis by wide-angle X-ray diffraction (WAXD), the decrease of Φ_{PL} can be elucidated and attributed to the ordering of the solid-state structures of **P1** and **P3**. To our surprise, Φ_{PL} of **P2** is preserved even in an ordered solid-state phase, and it is insensitive to the structural ordering. Structural analysis of **P2** revealed that the aliphatic dendritic side chains of **P2** effectively disturbing the intermolecular $\pi-\pi$ interactions among the conjugated backbones, which allows the preservation of Φ_{PL} in the environment with ordered packing of DP-PPV molecules. The results of time-resolved PL decay experiments also confirmed that **P2** possesses long-lived decay time because of excitons confined more effectively for emissive relaxation.

INTRODUCTION

Conjugated polymers have received considerable interest due to their potential applications as active materials in optoelectronic devices, such as light-emitting diodes,[1−3] thin film transistors,[4] and organic solar cells.[5] Among them, poly(phenylenevinylene) (PPV) and its derivatives have been one of the most extensively studied conjugated polymers because of their excellent optoelectronic properties and processability.[6] Although PPVs possess many advantages, poor solid-state photoluminescence (PL) efficiency (Φ_{PL}) has been a long-lasting challenge for the PPV derivatives. For most of the conjugated polymers, their Φ_{PL}s are substantially lower in the solid state than those in the solution state because of the formation of molecular aggregates. These molecular aggregates are lower-energy nonemissive sites in the polymer matrix, which can trap the excitation energy and quench the relaxation pathways of PL and electroluminescence (EL).[7,8] To minimize the formation of the aggregates and increase the Φ_{PL} in the solid state, various approaches, such as incorporation of meta-substitution in the polymer backbone,[9−12] polymer blends,[13,14] and introduction of pendant groups,[15−19] have been reported to control the $\pi-\pi$ interaction induced molecular aggregation.

Received: March 29, 2012
Revised: May 6, 2012
Published: May 16, 2012

   dx.doi.org/10.1021/ma300640n | *Macromolecules* 2012, 45, 4540−4549

Scheme 1. Synthetic Route of Homopolymers P1−P3

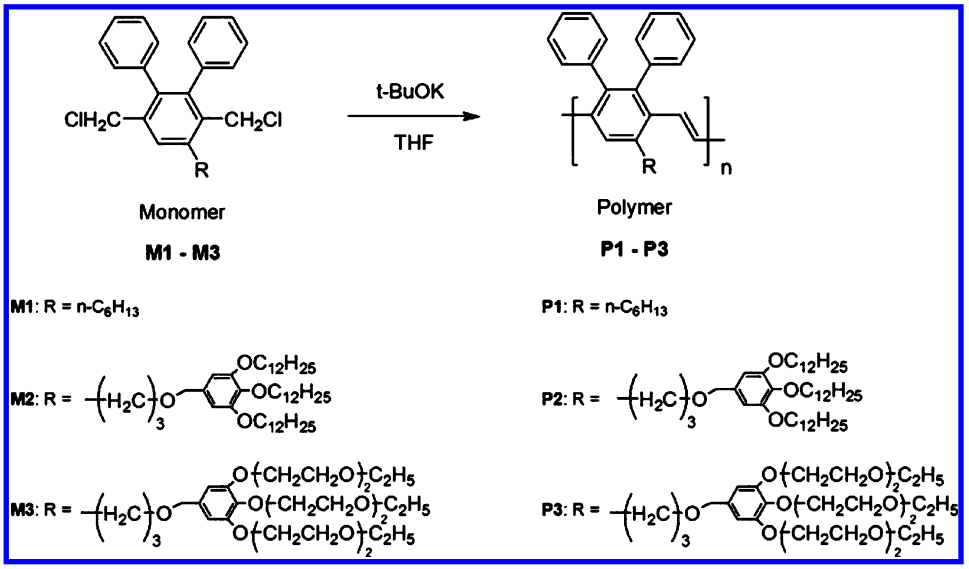

Among these researches, introducing of bulky pendant groups as polymer side chains has been demonstrated as a promising way to preserve the high Φ_{PL} in the solid state without changing the energy gaps of the parent polymer.[20,21] On the basis of this concept, PPV derivatives, poly(2,3-diphenyl-1,4-phenylenevinylene) (DP-PPV) and poly(2-dimethylphenylsilyl-1,4-phenylenevinylene) were synthesized and exhibits solid-state photoluminescence (PL) efficiency between 60 and 80%.[22,15] In addition, different substituents were introduced at C-5 position of the phenylene moieties of DP-PPV to not only further enhance the Φ_{PL}, but also to improve the solubility of the polymers.[22−24] Recently, we have also reported various types of novel DP-PPV-based copolymers with excellent polymer light emitting diode performance.[25−27]

Although the rational molecular designs of the PPVs have successfully enhanced the solid-state Φ_{PL} of PPVs, to the best of our knowledge, the relation between the solid-state phase structures and the Φ_{PL} of these highly emissive PPVs remains unexplored. The previous molecular designs used bulky substituents to minimize the intermolecular interactions among the conjugated chains, and avoid the formation of ordered structures in the solid state. However, it is still unclear if these amorphous phases of the PPVs are a thermodynamically stable phase and whether or not further ordering of the solid-state structure would decrease the Φ_{PL} of the materials. More importantly, it is of great interests to know if it is possible to preserve the Φ_{PL} even when the ordering process of the solid-state structure occurs. To reach in-depth understanding about this issue, a set of three DP-PPV derivatives (**P1**−**P3**) were synthesized via the Gilch polymerization as shown in Scheme 1. **P1** is the well-known poly(2,3-diphenyl-5-hexyl-*p*-phenylenevinylene), which demonstrates the solid-state Φ_{PL} over 60% in the as-casted film.[22] Its phase structure−photophysical property relation is carefully studied in this work. **P2** and **P3** are designed to bear hydrophobic and hydrophilic dendrons, respectively. Dendronized polymers also have been proved to efficiently restrain the aggregations of the polymer backbones,[28,29] and enhance the optical and electrical properties of conjugated polymers through reducing self-quenching process.[30−34] It is expected that the bulky dendritic pendants of **P2** and **P3** would block intermolecular interactions among the conjugated backbones. Furthermore, the hydrophilic dendrons of **P3** are purposely designed to study the effect of side-chain segregation on the phase structure and photophysical properties. The phase behaviors and phase structures were characterized with differential scanning calorimetry (DSC) and one-dimensional (1D) and two-dimensional (2D) wide-angle X-ray diffractometer (WAXD), and the photophysical properties were characterized with UV−vis absorption spectrophotometer, luminescence spectrometer, and time-resolved PL decay measurements. The structure−property relationships of **P1**−**P3** were investigated through the analysis and comparison of the phase structures solved from WAXD analysis and photophysical date measured from the spectroscopies.

EXPERIMENTAL SECTION

General Measurement and Characterization. ^{1}H and ^{13}C NMR spectra were measured with a Varian-300 MHz spectrometer. Gel permeation chromatography (GPC) data assembled from a Viscotek T50A Differential Viscometer and a LR125 Laser Refractometer. Three columns in series were used to measure the molecular weights of polymers relative to polystyrene standards. Thermal gravimetric analysis (TGA) was recorded on Perkin-Elmer Pyris under a nitrogen atmosphere at a heating rate of 10 °C/min. The differential scanning calorimetry (DSC) measurements were carried out utilizing a Perkin-Elmer Pyris I DSC with a mechanical refrigerator. The temperature and heat flow scales were calibrated at different heating and cooling rates (1−40 °C/min) using standard materials such as benzoic acid and indium. The one-dimensional (1D) wide-angle X-ray diffraction (WAXD) experiments were performed on a Philips X'Pert Pro diffractometer with a 3 kW ceramic tube as the X-ray source (Cu K_α) and an X'celerator detector. The sample stage was set horizontally. The reflection peak positions were calibrated with silicon powder (2θ > 15°) and silver behenate (2θ< 10°). A temperature control unit (Paar Physica TCU 100) in conjunction with the diffractometer was utilized to study the structure evolutions as a function of temperature. The heating and cooling rates in the WAXD experiments were 1.5 °C/min. Two-dimensional (2D) WAXD patterns were obtained using a Bruker D8Discover diffractometer with GADDS as a 2D detector. Again, calibration was conducted using silicon powder and silver behenate. Samples were mounted on the sample stage, and the point-focused X-ray beam was aligned both perpendicular and parallel to the mechanical shearing direction. The 2D diffraction patterns were recorded in a transmission mode at room temperature. UV−vis absorption spectra were obtained with an HP

dx.doi.org/10.1021/ma300640n | *Macromolecules* 2012, 45, 4540−4549

Scheme 2. Synthetic Route of Monomers M2 and M3

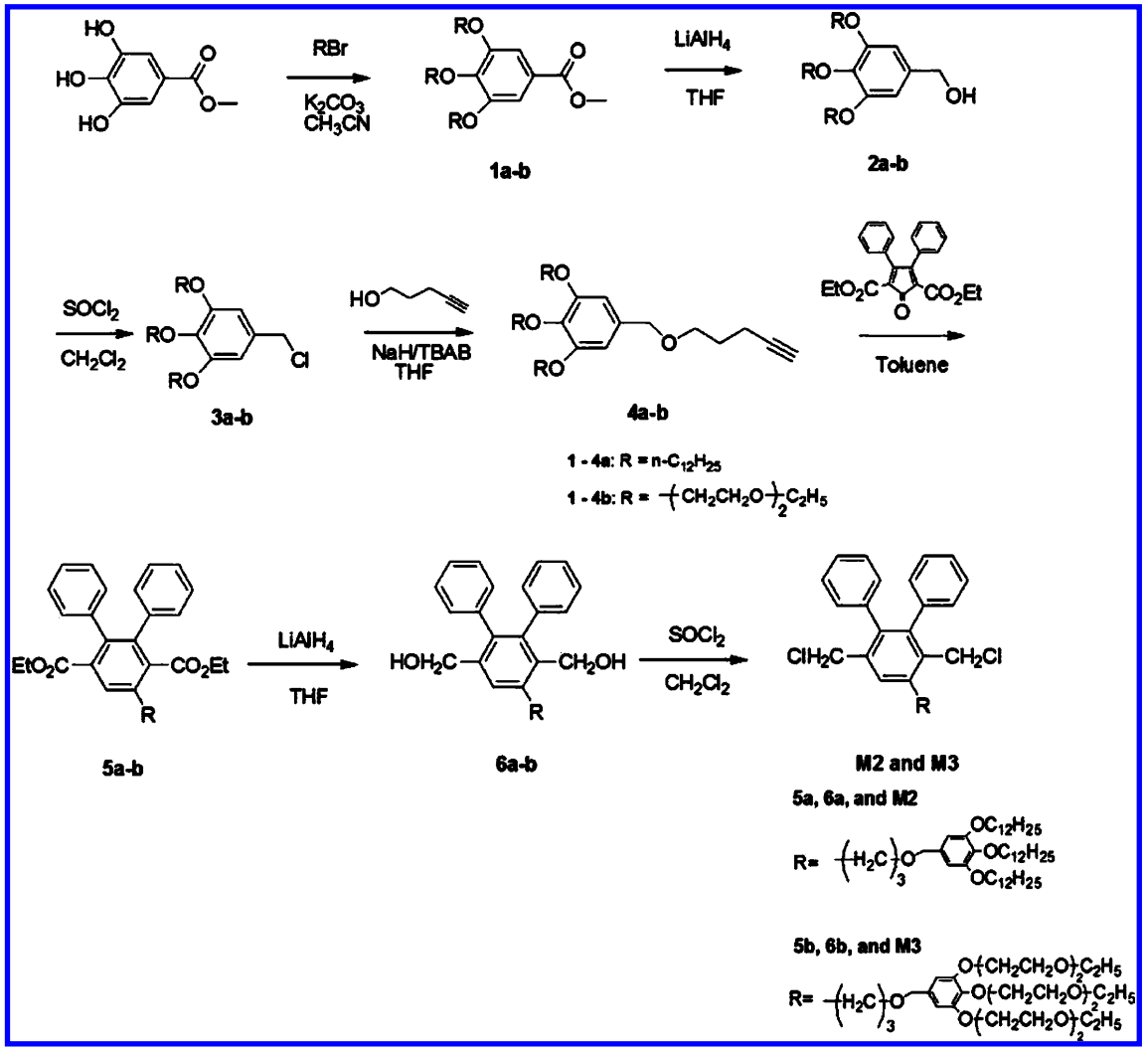

8453 diode array spectrophotometer. PL emission spectra were obtained using ARC SpectraPro-150 luminescence spectrometer. The photoluminescence (quantum) efficiency were measured according to the previous literatures.[10,20,34] For example, the polymer films for solid-state PL measurement were prepared by spin-cast on quartz substrates. The thickness of the films was controlled to ensure the intensity of their absorbance was between 0.08 and 0.10. The relative PL efficiency of films were estimated by using $\Phi_s/\Phi_r = (A_r/A_s)(F_s/F_r)(n_s^2/n_r^2) \approx (A_r/A_s)(F_s/F_r)$, assuming the same refractive index for polymer films. Here Φ_r, A_r, and F_r are PL efficiency, absorbance at excitation wavelength, and emission integration area for the reference, while A_s and F_s are absorbance and emission integration for the sample film.[10] The PL efficiency of polymer film was calculated by assuming the efficiency of the reference polyfluorene thin film to be 0.55.[34] The transient photoluminescence experiments have been achieved with a homemade, time-resolved confocal microscope setup. Excitation at 400 nm was provided by a Spectra-Physics Hurricane X laser system (82 fs, 1 kHz). The mean pump power impinging on samples was kept well below 0.1 mW with density filters to minimize sample photobleaching and annihilation processes. The collected emission was temporally detected with a streak camera (Hamamatsu C7700) coupled to an imaging spectrograph.

Sample Preparation. For DSC experiments, a typical mass of 5 mg was encapsulated in a sealed aluminum pan with the pan weight identically matched to the reference pan. For 1D WAXD powder experiments, the samples were cast from chloroform solution and dried at room temperature under a vacuum. The films were then kept under vacuum for several days. For 2D WAXD experiments, the oriented samples were prepared by mechanically shearing the **P1**, **P2**, and **P3** polymers at 320, 180, and 200 °C.

Synthesis of Monomers. All reagents and chemicals were purchased from commercial sources (Aldrich, Lancaster, or TCI) and used without further purification. Tetrahydrofuran (THF) was dried by distillation from sodium/benzophenone. The synthetic route of **P1**−**P3** are shown in Scheme 1, and the synthetic routes for monomers **M2** and **M3** are shown in Scheme 2. Compounds **1a**, **1b**, **2a**, **2b**, **3a**, and **3b** in Scheme 2 and **M1** in Scheme 1 were synthesized according to previous literature.[22,35,36]

3,4,5-Tris(dodecyloxy)-1-benzyloxypent-4-yne (4a). Into a two-neck round-bottom flask was added sodium hydride (0.72 g, 30.0 mmol) in the presence of 0.1 equiv of tetrabutylammonium bromide. Dendritic chloride **3a** (6.8 g, 10.0 mmol) in THF (50 mL) and pent-4-yn-1-ol (2.5 g, 30.0 mmol) were added dropwise subsequently. The mixture was refluxed for 12 h under nitrogen atmosphere. The excess of sodium hydride was quenched with water (2 mL) in an ice bath. After evaporating the solvent, the crude product was dissolved in 100 mL of ethyl acetate and extracted with brine (200 mL) twice. The combined organic layer was dried over $MgSO_4$. After removal the solvent under reduced pressure, the residue was purified by column chromatography on silica gel [ethyl acetate/hexane = 1/40 (v/v)] to give a colorless liquid **4a**.(5.2 g, 72%).

^{1}H NMR ($CDCl_3$, δ, ppm): 0.86−0.94 (m, 9H), 1.20−1.46 (m, 54H), 1.70−1.87 (m, 8H), 1.94 (s, 1H), 2.29−2.35 (t, 2H), 3.54−3.58 (t, 2H), 3.90−3.99 (m, 6H), 4.40 (s, 2H), 6.52 (s, 2H). ^{13}C NMR

dx.doi.org/10.1021/ma300640n | Macromolecules 2012, 45, 4540−4549

($CDCl_3$, δ, ppm): 14.10, 15.30, 22.68, 26.10, 28.62, 29.36, 29.41, 29.65, 29.69, 29.75, 30.31, 31.92, 68.45, 68.59, 69.05, 73.25, 73.38, 83.93, 106.07, 133.42, 137.56, 153.12. MS (EI, $C_{48}H_{86}O_4$): calcd, 727.19; found, 726.

3,4,5-Tris(2-(2-ethoxyethoxy)ethoxy)-1-benzyloxypent-4-yne (4b). Into a two-neck round-bottom flask was added sodium hydride (1.27 g, 52.8 mmol) in the presence of 0.1 equiv of tetrabutylammonium bromide. Dendritic chloride **3b** (9.2 g, 17.6 mmol) in THF (50 mL) and pent-4-yn-1-ol (4.5 g, 52.8 mmol) were added dropwise subsequently. The mixture was refluxed for 12 h under nitrogen atmosphere. The excess of sodium hydride was quenched with water (2 mL) in an ice bath. After evaporating the solvent, the crude product was dissolved in 100 mL of ethyl acetate and extracted with brine (200 mL) twice. The combined organic layer was dried over $MgSO_4$. After removal the solvent under reduced pressure, the residue was purified by column chromatography on silica gel [ethyl acetate/hexane = 2/1 (v/v)] to give a yellow liquid **4b**. (8.5 g, 85%)

^{1}H NMR ($CDCl_3$, δ, ppm): 1.14−1.23 (t, 9H), 1.80−1.86 (m, 2H), 1.95 (s, 1H), 2.31−2.34 (t, 2H), 3.47−3.87 (m, 28H), 4.12−4.18 (m, 6H), 4.39 (s, 2H), 6.57 (s, 2H). ^{13}C NMR ($CDCl_3$, δ, ppm): 15.14, 15.26, 28.55, 66.64, 68.56, 68.76, 69.70, 69.87, 69.90, 70.49, 70.52, 70.86, 72.29, 72.96, 83.85, 106.98, 133.91, 137.68, 152.59. MS (EI, $C_{30}H_{50}O_{10}$): calcd, 570.71; found, 570.

Diethyl 2,3-diphenyl-5-(3,4,5-tris(dodecyloxy)-1-benzyloxypropyl) terephthalate (5a). A solution of 2,5-bis(ethoxycarbonyl)-3,4-diphenylcyclopentadienone (2.7 g, 7.1 mmol) and **4a** (5.2 g, 7.1 mmol) in 20 mL of toluene was refluxed for 12 h. The mixture was then cooled to room temperature. After removal of the toluene under reduced pressure, the residue was purified by column chromatography on silica gel [ethyl acetate/hexane = 1/10 (v/v)] to produce an orange oil **5a**. (6.2 g, 81%)

^{1}H NMR ($CDCl_3$, δ, ppm): 0.80−1.00 (m, 15H), 1.06−1.44 (m, 54H), 1.67−1.83 (m, 6H), 1.98−2.03 (m, 2H), 2.77−2.82 (t, 2H), 3.50−3.54 (t, 2H), 3.85−3.99 (m, 10H), 4.40 (s, 2H), 6.53 (s, 2H), 6.91−7.09 (m, 10H), 7.67 (s, 1H). ^{13}C NMR ($CDCl_3$, δ, ppm): 13.52, 14.09, 22.67, 26.11, 29.35, 29.37, 29.43, 29.64, 29.69, 29.73, 30.07, 30.32, 31.03, 31.90, 61.03, 69.05, 69.46, 73.08, 73.37, 106.01, 126.50, 126.83, 127.19, 127.22, 129.08, 129.77, 130.11, 133.52, 133.59, 137.21, 137.53, 137.90, 138.16, 138.71, 138.89, 139.73, 153.12, 168.49, 168.67. MS (FAB, $C_{70}H_{106}O_8$): calcd, 1075.59; found, 1075.

Diethyl 2,3-diphenyl-5-(3,4,5-tris(2-(2-ethoxyethoxy)-ethoxy)-1-benzyloxypropyl) terephthalate (5b). A solution of 2,5-bis(ethoxycarbonyl)-3,4-diphenylcyclopentadienone (3.8 g, 10.0 mmol) and **4b** (5.7 g, 10.0 mmol) in 20 mL of toluene was refluxed for 12 h. The mixture was then cooled to room temperature. After removal the toluene under reduced pressure, the residue was purified by column chromatography on silica gel [ethyl acetate/hexane = 3/1 (v/v)] to produce an orange oil **5b**. (7.5 g, 82%)

^{1}H NMR ($CDCl_3$, δ, ppm): 0.79−0.88 (t, 6H), 1.11−1.25 (t, 9H), 1.98−2.05 (m, 2H), 2.78−2.83 (t, 2H), 3.44−4.00 (m, 30H), 4.09−4.19 (m, 6H), 4.40 (s, 2H), 6.59 (s, 2H), 6.92−7.10 (m, 10H), 7.68 (s, 1H). ^{13}C NMR ($CDCl_3$, δ, ppm): 14.12, 15.14, 29.27, 31.49, 60.92, 66.62, 68.73, 69.40, 69.70, 69.82, 69.88, 70.51, 70.81, 72.31, 72.74, 105.96, 126.59, 126.85, 127.18, 127.27, 129.38, 129.77, 130.13, 133.53, 133.59, 137.26, 137.53, 137.90, 138.16, 138.71, 139.39, 140.17, 152.55, 168.34, 168.87. MS (FAB, $C_{52}H_{70}O_{14}$): calcd, 919.10; found, 919.

2,3-Diphenyl-5-(3,4,5-tris(dodecyloxy)-1-benzyloxypropyl)-1,4-bis(hydroxymethyl)benzene (6a). A solution of **5a** (6.0 g, 5.6 mmol) in dry THF (40 mL) was added dropwise under nitrogen atmosphere to a stirred suspension of $LiAlH_4$ (2.2 g, 56.0 mmol) in dry THF (20 mL) cooled to 0 °C in an ice bath. The reaction mixture was stirred and refluxed for 12 h. The excess of hydride was quenched under cooling in an ice bath with 15% NaOH(aq) (2 mL) followed by H_2O (10 mL). The THF was removed by evaporation and the resulting mixture was dissolved in 100 mL of ethyl acetate and extracted with brine (200 mL) twice. The organic phase was then dried over $MgSO_4$, evaporated, and purified with column chromatography [silica gel, ethyl acetate/hexane = 1/3 (v/v)) as eluent] to yield **6a** as a white solid (4.9 g, 89%)

^{1}H NMR ($CDCl_3$, δ, ppm): 0.83−0.88 (t, 9H), 1.17−1.43 (m, 54H), 1.69−1.89 (m, 6H), 2.03−2.08 (m, 2H), 2.94−3.00 (t, 2H), 3.55−3.59 (t, 2H), 3.89−3.97 (m, 6H), 4.38 (s, 2H), 4.40 (s, 2H), 4.42 (s, 2H), 6.47 (s, 2H), 6.89−7.12 (m, 10H), 7.59 (s, 1H). ^{13}C NMR ($CDCl_3$, δ, ppm): 14.08, 22.68, 26.12, 29.22, 29.35, 29.45, 29.64, 29.69, 29.74, 30.07, 30.32, 31.04, 31.91, 59.41, 63.43, 69.06, 69.53, 73.16, 73.98, 105.98, 126.60, 126.84, 127.33, 127.56, 130.09, 130.29, 133.66, 133.91, 136.52, 137.46, 138.17, 138.73, 139.80, 140.16, 141.47, 153.16. MS (FAB, $C_{66}H_{102}O_6$): calcd, 991.51; found, 991.

2,3-Diphenyl-5-(3,4,5-tris(2-(2-ethoxyethoxy)ethoxy)-1-benzyloxypropyl)-1,4-bis(hydroxymethyl)benzene (6b). A solution of **5b** (5.4 g, 5.9 mmol) in dry THF (40 mL) was added dropwise under nitrogen atmosphere to a stirred suspension of $LiAlH_4$ (2.3 g, 59.0 mmol) in dry THF (20 mL) cooled to 0 °C in an ice bath. The reaction mixture was stirred and refluxed for 12 h. The excess of hydride was quenched under cooling in an ice bath with 15% NaOH(aq) (2 mL) followed by H_2O (10 mL). The THF was removed by evaporation and the resulting mixture was dissolved in 100 mL of ethyl acetate and extracted with brine (200 mL) twice. The organic phase was then dried over $MgSO_4$, evaporated, and purified with column chromatography [silica gel, ethyl acetate as eluent] to yield **6b** as a colorless oil (3.9 g, 75%).

^{1}H NMR ($CDCl_3$, δ, ppm): 1.12−1.27 (t, 9H), 2.04−2.09 (m, 2H), 2.97−3.02 (t, 2H), 3.45−3.87 (m, 26H), 4.13−4.19 (m, 6H), 4.40 (s, 2H), 4.43 (s, 2H), 4.44 (s, 2H), 6.63 (s, 2H), 6.93−7.15 (m, 10H), 7.46 (s, 1H). ^{13}C NMR ($CDCl_3$, δ, ppm): 15.10, 15.14, 29.27, 31.49, 59.47, 63.33, 66.62, 68.73, 69.40, 69.70, 69.82, 69.88, 70.51, 70.81, 72.31, 72.74, 107.09, 126.34, 127.35, 127.50, 128.08, 129.98, 130.16, 133.98, 135.68, 137.68, 138.39, 138.43, 139.01, 139.64, 140.92, 142.57, 152.57. MS (FAB, $C_{48}H_{66}O_{12}$): calcd, 835.03; found, 835.

2,3-Diphenyl-5-(3,4,5-tris(dodecyloxy)-1-benzyloxypropyl)-1,4-bis(chloromethyl)benzene (M2). Into two-neck round-bottom flask was added **6a** (4.6 g, 4.6 mmol) dissolved in 20 mL of CH_2Cl_2. Then 1 M $SOCl_2$ (18.6 mL, 18.6 mmol) was added dropwise via a dropping funnel. The reaction was stirred at room temperature for 2 h. The solvent was removed and the crude product was redissolved in CH_2Cl_2, washed twice with brine and dried over $MgSO_4$. Evaporation of the solvent yielded the crude product, which was purified by column chromatography [silica gel, ethyl acetate/hexane = 1/30 (v/v)]. The pure fractions were collected, and after evaporation resulted in a viscous oil (2.0 g, 42%)

^{1}H NMR ($CDCl_3$, δ, ppm): 0.84−0.88 (t, 9H), 1.18−1.44 (m, 54H), 1.67−1.82 (m, 6H), 2.05−2.10 (m, 2H), 2.95−3.00 (t, 2H), 3.58−3.62 (t, 2H), 3.89−3.98 (m, 6H), 4.31 (s, 2H), 4.38 (s, 2H), 4.45 (s, 2H), 6.56 (s, 2H), 6.96−7.18 (m, 10H), 7.46 (s, 1H). ^{13}C NMR ($CDCl_3$, δ, ppm): 14.10, 22.68, 26.10, 29.05, 29.35, 29.42, 29.64, 29.69, 29.74, 30.32, 31.05, 31.91, 41.66, 44.60, 69.06, 69.53, 73.22, 73.38, 106.05, 126.69, 126.74, 127.36, 127.46, 130.09, 130.29, 133.46, 133.91, 136.01, 137.56, 138.17, 138.67, 139.80, 141.43, 143.20, 153.16. MS (FAB, $C_{66}H_{100}Cl_2O_4$): calcd, 1028.40; found, 1027. Anal. Calcd for $C_{66}H_{100}Cl_2O_4$: C, 77.08; H, 9.80. Found: C, 77.18; H, 9.89.

2,3-Diphenyl-5-(3,4,5-tris(2-(2-ethoxyethoxy)ethoxy)-1-benzyloxypropyl)-1,4-bis(chloromethyl)benzene (M3). Into a two-neck round-bottom flask was added **6b** (3.4 g, 4.0 mmol) dissolved in 20 mL of CH_2Cl_2. Then, 1 M $SOCl_2$ (16.0 mL, 16.0 mmol) was added dropwise via a dropping funnel. The reaction was stirred at room temperature for 2 h. The solvent was removed and the crude product was redissolved in CH_2Cl_2, washed twice with brine and dried over $MgSO_4$. Evaporation of the solvent yielded the crude product, which was purified by column chromatography [silica gel, ethyl acetate/hexane = 1/1 (v/v)]. The pure fractions were collected, and after evaporation resulted in a viscous oil (2.2 g, 63%)

^{1}H NMR ($CDCl_3$, δ, ppm): 1.14−1.28 (t, 9H), 2.06−2.17 (m, 2H), 2.96−3.01 (t, 2H), 3.49−3.88 (m, 26H), 4.13−4.19 (m, 6H), 4.33 (s, 2H), 4.40 (s, 2H), 4.46 (s, 2H), 6.62 (s, 2H), 6.98−7.18 (m, 10H), 7.47 (s, 1H). ^{13}C NMR ($CDCl_3$, δ, ppm): 15.15, 29.05, 31.05, 41.69, 44.60, 66.65, 68.82, 69.59, 69.74, 69.88, 69.92, 70.54, 70.87, 72.33, 72.94, 106.99, 126.69, 126.75, 127.28, 127.37, 127.46, 130.11, 130.21, 130.29, 133.90, 133.98, 136.02, 138.19, 138.67, 141.40, 143.21, 152.65.

MS (FAB, $C_{48}H_{64}Cl_2O_{10}$): calcd, 871.92; found, 871. Anal. Calcd for $C_{48}H_{64}Cl_2O_{10}$: C, 66.12; H, 7.40. Found: C, 65.98; H, 7.23.

Synthesis of Polymers. Scheme 1 outlines the synthetic route of polymers **P1**−**P3**.

P1. To a solution of **M1** (1.95 g, 4.74 mmol) in THF (300 mL) and potassium *tert*-butoxide (8.51 g, 75.8 mmol) in THF (174 mL) was added. The resulting mixture was stirred at room temperature for 12 h under a nitrogen atmosphere. A solution of 2,6-di-*tert*-butylphenol (6 equiv) as end-capping agent in THF (20 mL) was then added and stirred for 6 h. The resulting mixture was poured into methanol, and the precipitate was filtered off and washed with water. The resulting polymer was dissolved in THF, precipitated again in methanol, and washed by Soxhlet extraction with methanol for 2 days. After drying under vacuum for 24 h, the polymer was obtained as a yellow solid (0.92 g, 55%).

^{1}H NMR ($CDCl_3$, δ, ppm): 0.76−0.89 (m, 3H), 1.20−1.27 (m, 6H), 2.17−2.53 (m, 2H), 3.40−3.49 (m, 2H), 5.77−6.06 (m, 2H), 6.25−7.00 (m, 10H), 7.60 (s, 1H). GPC (THF, polystyrene standard): M_n = 182 kDa, M_w = 418 kDa, PDI = 2.30.

P2. To a solution of **M2** (0.96 g, 0.94 mmol) in THF (70 mL) and potassium *tert*-butoxide (1.68 g, 15.0 mmol) in THF (24 mL) was added. The resulting mixture was stirred at room temperature for 12 h under a nitrogen atmosphere. A solution of 2,6-di-*tert*-butylphenol (6 equiv) as end-capping agent in THF (20 mL) was then added and stirred for 6 h. The resulting mixture was poured into methanol, and the precipitate was filtered off and washed with water. The resulting polymer was dissolved in THF, precipitated again in methanol, and washed by Soxhlet extraction with methanol for 2 days. After drying under vacuum for 24 h, the polymer was obtained as a yellow solid (0.45 g, 50%).

^{1}H NMR ($CDCl_3$, δ, ppm): 0.86−0.97 (m, 9H), 1.06−1.44 (m, 54H), 1.72−1.88 (m, 6H), 2.47−2.58 (m, 2H), 3.21−3.43 (m, 2H), 3.82−4.02 (m, 8H), 4.23−4.32 (m, 2H), 5.99−6.05 (m, 2H), 6.30−6.50 (m, 2H), 6.58−7.18 (m, 10H), 7.60 (s, 1H).

GPC (THF, polystyrene standard): M_n = 135 kDa, M_w = 389 kDa, PDI = 2.88.

P3. To a solution of **M3** (1.15 g, 1.32 mmol) in THF (100 mL) and potassium *tert*-butoxide (2.37 g, 21.1 mmol) in THF (32 mL) was added. The resulting mixture was stirred at room temperature for 12 h under a nitrogen atmosphere. A solution of 2,6-di-*tert*-butylphenol (6 equiv) as end-capping agent in THF (20 mL) was then added and stirred for 6 h. The resulting mixture was poured into methanol, and the precipitate was filtered off and washed with water. The resulting polymer was dissolved in THF, precipitated again in methanol, and washed by Soxhlet extraction with methanol for 2 days. After drying under vacuum for 24 h, the polymer was obtained as a yellow solid (0.43 g, 41%).

^{1}H NMR ($CDCl_3$, δ, ppm): 0.98−1.19 (m, 9H), 2.40−2.46 (m, 2H), 3.20−3.28 (m, 2H), 3.45−3.72 (m, 26H), 3.81−4.11 (m, 8H), 4.31−4.41 (m, 2H), 6.01−6.05 (m, 2H), 6.44−6.47 (m, 2H), 6.54−7.15 (m, 10H), 7.60 (s, 1H).

GPC (THF, polystyrene standard): M_n = 58.8 kDa, M_w = 147 kDa, PDI = 2.50.

RESULTS AND DISCUSSION

Synthesis. Scheme 2 outlines the synthetic route for the monomers. Dendritic benzyl chlorides **3a**,**b** were prepared through the sequential $LiAlH_4$ reduction and $SOCl_2$-mediated chlorination of dendritic benzoate **1a**,**b**. Substitution of the chloro functional group of the corresponding dendritic chlorides with pent-4-yn-1-ol in the presence of sodium hydride and tetrabutylammonium bromide (TBAB) afforded compound **4a**,**b**. The Diels−Alder reaction of 2,5-bis-(ethoxycarbonyl)-3,4-diphenylcyclopentadienone with **4a**,**b** gives **5a**,**b** in high yields. **5a**,**b** are then reduced with $LiAlH_4$ to give **6a**,**b** and then reacted with $SOCl_2$ in methylene chloride to produce the monomers, **M2** and **M3**. The obtained monomers were then polymerized via Gilch route to obtain DP-PPV derivatives, **P1**−**P3** (Scheme 1) in good yields. Yields, molecular weight and polydispersity index (PDI) of resulting polymers are reported in Table 1. Because of the substituents at C-5 position of the phenylene moieties, **P1**−**P3** are highly soluble in common organic solvents, such as chloroform, toluene, and chlorobenzene and can be polymerized to relatively high molecular weight. Number-average molecular weights (M_n) of the polymers are in the range from 59 to 180 kDa (Table 1). Transparent and self-standing films can be cast from their solutions. **P2** and **P3** show lower yield and molecular weight than that of **P1**, which implies that the bulkier pendant groups may result in larger steric hindrance and a less efficient polymerization process.

Table 1. Molecular Weights and Thermal Properties of Polymers P1−P3

polymer	yield (%)	M_n (kDa)	M_w (kDa)	PDI (M_w/M_n)	T_i (°C)	T_d (°C)
P1	55	182	418	2.30	308	419
P2	50	135	389	2.88	169	347
P3	41	58.8	147	2.50	189	318

Thermal properties. In the TGA measurements, the 5% weight loss temperatures of **P1**−**P3** were observed above 310 °C at a heating rate of 10 °C/min (Figure S7, Supporting Information), suggesting the good thermal stability of the polymers. Figure 1 shows the DSC thermal diagrams of **P1**−**P3**, which recorded the cooling scan from their isotropic (*I*) melts and the subsequent heating scans at 10 °C/min. The *I* phases of **P1**−**P3** were confirmed by the amorphous halos observed in their wide-angle X-ray diffraction (WAXD) patterns (Figure S8, Supporting Information). During the cooling, all the polymers show a *I* phase to an ordered phase transition. The transition temperatures are found at 234 °C (latent heat (ΔH) = −6.22 J/g) for **P1**, 139 °C (ΔH = −2.93 J/g) for **P2**, and 126 °C (ΔH = −2.31 J/g) for **P3**. Upon the subsequent heating, the endothermic thermal transitions, which represents the isotropization of **P1**−**P3** were observed at temperature (T_i) of 308 °C (ΔH = 6.23 J/g), 169 °C (ΔH =

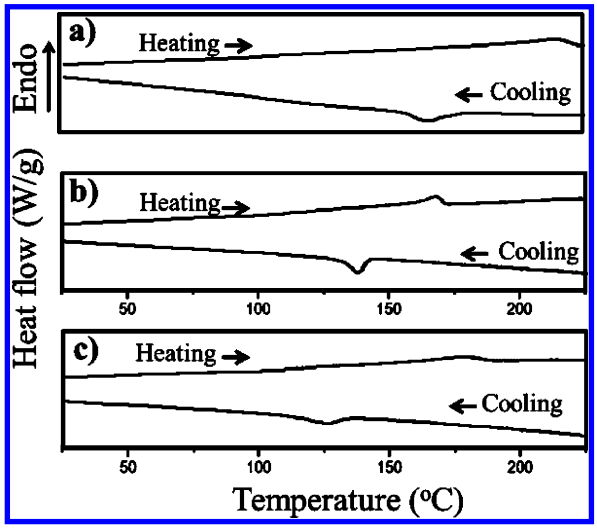

Figure 1. DSC thermal diagrams of (a) **P1**, (b) **P2** and (c) **P3** at a scan rate of 10 °C/min. The two thermal scans of each sample include a cooling scan from the *I* phase and the subsequent heating scan.

dx.doi.org/10.1021/ma300640n | *Macromolecules* 2012, 45, 4540−4549

2.96 J/g) and 189 °C (ΔH = 2.35 J/g), respectively. The nearly identical latent heats during the cooling and heating scans of each polymer indicate that the three DP-PPV derivatives all exhibit an enantiotropic phase behavior. The much lower T_is of **P2** and **P3** compared to that of **P1** indicates that the flexible dendritic side chains of **P2** and **P3** significant decreases the isotropization temperature. A smaller supercooling was also observed in the phase transition of **P2**, suggesting a smaller kinetic energy barrier for **P2** to transform from its *I* phase to an ordered phase.

Optical Properties. Figure 2 shows the UV−vis absorption and PL emission spectra of polymers in chloroform and thin

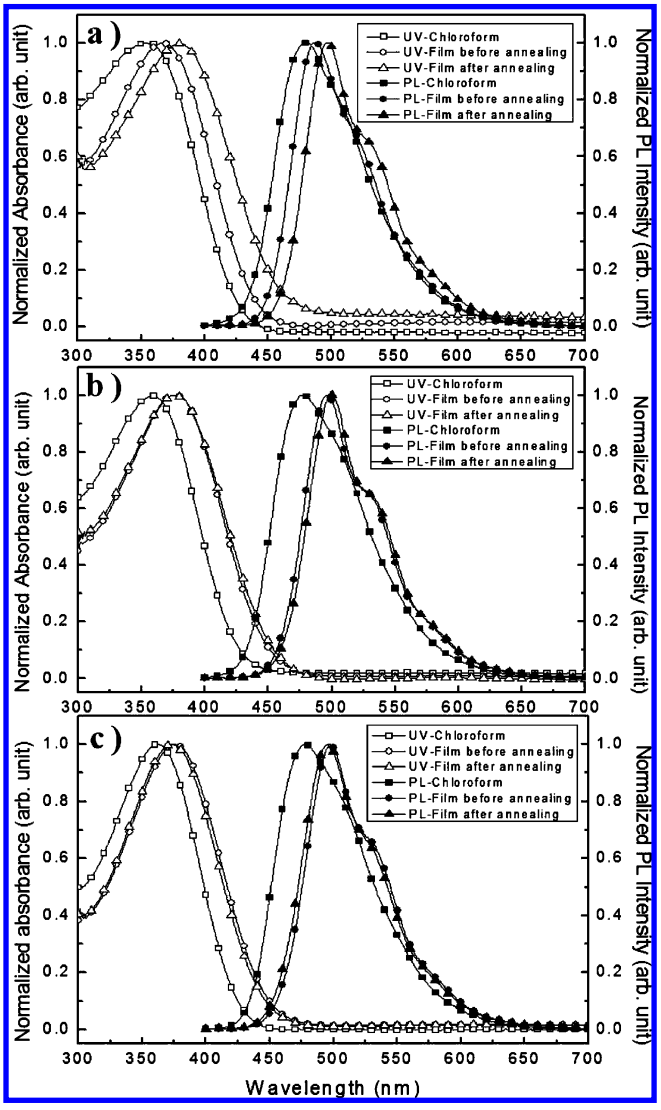

Figure 2. UV−vis and PL spectra of (a) **P1**, (b) **P2** and (c) **P3**.

film state. Table 2 summarizes the UV−vis absorption maxima and PL emission maxima of all polymers in different states. In the chloroform solution, the absorption maxima of **P1**−**P3** are located in the range from 352 to 362 nm, and the PL emission maxima are located in the range from 477 to 481 nm, which is attributed to the π−π^* transition of the polymers. Thus, the modification on the side chain structures of **P1**−**P3** shows limited effects on their energy gaps. Red shift of the absorption and PL maxima were observed in the thin-films of all the polymers, which indicates a closer intermolecular distance and stronger intermolecular interactions among the polymer chains in the thin-film state. As shown in Table 2, in the chloroform solution, **P2** possesses a remarkably high Φ_{PL}, 86%, and both the Φ_{PL}s of **P2** and **P3** are further enhanced from their predecessor, **P1**. These results demonstrate that the incorporation of appropriate dendritic moieties as polymer side chains can lead to less chain aggregation, and higher Φ_{PL} in the DP-PPV derivatives. Accompanying with the decrease of intermolecular distance in the thin-film state, the Φ_{PL}s of **P1** and **P3** dropped to 65% and 63%, while **P2** keeps its Φ_{PL} at 77%. To further investigate how the structural ordering in the thin-film affects Φ_{PL}, the thin films of **P1**−**P3** were thermally treated according to their DSC thermograms. These polymer films were first heated to temperature above the T_i of the corresponding polymer, and then cooled slowly to room temperature under a nitrogen atmosphere to allow the structural development of each polymer. After the thermal treatment, the Φ_{PL}s of **P1** and **P3** decreased significantly to 33% and 38%. However, the Φ_{PL} of **P2** was kept at remarkable high value of 71%. Therefore, it is obvious the Φ_{PL} of **P2** is much less sensitive to the structural ordering in the solid state, and the aliphatic dendritic side chains provides the polymer a better ability to preserve its Φ_{PL} in the solid state.

Time-resolved PL decay experiments are shown in Figure 3. The PL lifetimes of the three polymers in chloroform solution has no obvious difference. However, in the thin-film state, the PL lifetime of **P2** is longer than those of **P1** and **P3** even after thermal treatment. Therefore, the excitons generated in **P2** are more effectively confined for emissive relaxation, which results in a higher Φ_{PL} and longer lifetime.[37−39]

Analysis of 1D-WAXD and 2D-WAXD Patterns. To gain insights about the phase structures of **P1**−**P3** and identify the structure−property relationships of these polymers, a series of 1D WAXD patterns have been acquired as shown in Figure 4. To relate the Φ_{PL} and the lifetime of the as-casted samples and thermally treated samples to their phase structures, two kinds of solid samples of **P1**−**P3** were prepared. The "dried samples" were made by completely evaporating the solvent (chloroform) from the respective polymer solutions, and are used to identify the possible lyotropic ordered structure in the as-casted films formed during the solvent evaporation. The thermally treated samples were prepared via cooling the individual polymer melts to room temperature, and are used to study the corresponding structural changes, which result in the significant drops in the Φ_{PL} of the thermally treated **P1** and **P3**. The 1D WAXD patterns of the dried samples are shown in the bottom of Figures 4a−c. Diffuse halos are observed for the dried samples of **P1** and **P3**. The halos indicates that **P1** and **P3** were trapped in a relatively amorphous state with random chain orientations during the solvent evaporation process. On the other hand, the dried sample of **P2** shows a Bragg diffractions located at 2θ of 2.38° (*d*-spacing: 3.71 nm), and an amorphous halo centered at 19.61° (*d*-spacing: 0.45 nm). The Bragg diffraction in the low 2θ angle region represents an ordered packing of **P2** molecules at a length scale of a **P2** molecular dimension (*vide infra*), while the halo in the high 2θ angle region can be attributed to a short-range order at the segmental level within molecules.[40] The ordered phase of **P2** is therefore a mesophase. The 1D WAXD patterns of the dried samples indicate that the solvent evaporation process allows the formation of the lyotropic mesophase of **P2**, but results in amorphous phases and random chain packing of **P1** and **P3**. Since the structure evolutions of **P1**−**P3** were clearly observed in the DSC measurements,

dx.doi.org/10.1021/ma300640n | *Macromolecules* 2012, 45, 4540−4549

Table 2. Optical Properties of Polymers P1−P3

	UV−vis (nm)			PL (nm)		
polymer	$CHCl_3$	Film-1[a]	Film-2[b]	$CHCl_3$	Film-1[a]	Film-2[b]
P1	352	367	381	481 (0.80)[c]	488 (0.65)[d]	498 (0.33)[d]
P2	359	377	376	477 (0.86)	496 (0.77)	501 (0.71)
P3	362	375	374	477 (0.82)	497 (0.63)	497 (0.38)

[a]Film-1 was treated before thermal annealing. [b]Film-2 was treated after thermal annealing. [c]Solution PL quantum efficiency were measured in $CHCl_3$, relative to 9,10-diphenylanthracene (Φ_{PL} = 0.90). [d]PL quantum efficiency were estimated relative to polyfluorene thin film as a standard (Φ_{PL} = 0.55).

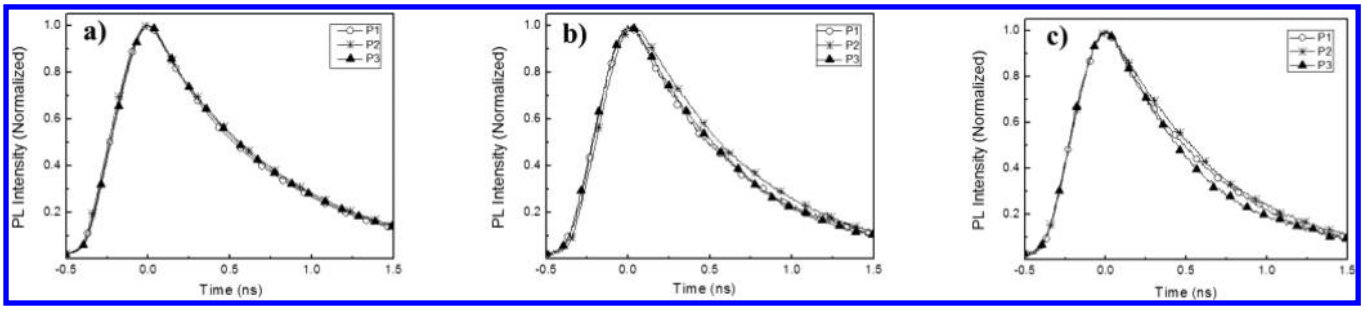

Figure 3. Time-resolved PL decay of polymers (a) in $CHCl_3$ solution, (b) in film state before thermal treatment, and (c) in film state after thermal treatment following 400 nm excitation.

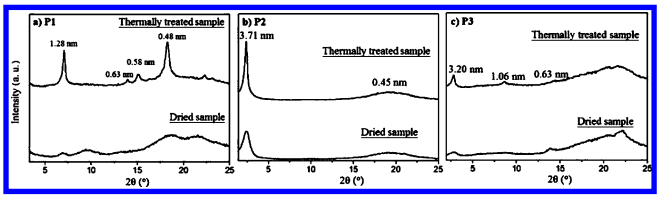

Figure 4. Set of 1D WAXD patterns of (a) **P1**, (b) **P2** and (c) **P3**. The bottom patterns in each figure are the 1D WAXD patterns of the dried samples recorded at 30 °C. The top patterns are the 1D WAXD patterns of the thermally treated samples, which were cooled from the *I* phases to room temperature, and recorded at 30 °C.

WAXD pattern of thermal treated samples of **P1**−**P3** were further investigated. The 1D WAXD patterns of these samples are shown as the top patterns in Figures 4a-c. Bragg diffractions were observed for the thermally treated **P1** and **P3**, representing the formation of ordered phases of **P1** and **P3** during cooling the samples from their melts. The diffraction peaks of **P1** are found at 2θ = 6.89°, 14.01°, 15.32°, and 18.35° which corresponds to *d*-spacings of 1.28, 0.63, 0.58, and 0.48 nm. For **P3**, the diffraction peaks are found at 2θ = 2.76°, 8.32°, and 14.05°, which corresponds to *d*-spacings of 3.20, 1.06, and 0.63 nm. Interesting, in Figure 4b, cooling **P2** from its melt only leads to a stronger and sharper diffraction peak located at identical 2θ angle (2.38°). Therefore, the ordered structures observed in the dried sample and the thermally treated sample

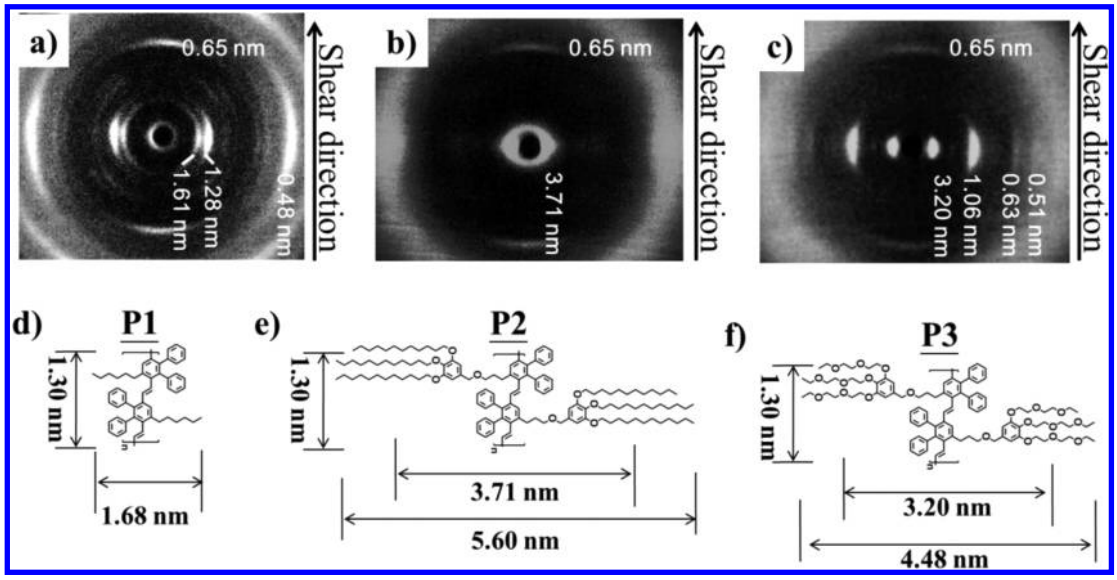

Figure 5. 2D WAXD patterns of the ordered phases of (a) **P1**, (b) **P2**, and (c) **P3** after shearing. Solid arrow indicates the direction of mechanical shearing force applied on the sample. The incident X-ray beam was along the normal direction of the 2D patterns. Schematic representations of the molecular dimensions along the chain and the lateral directions are illustrated in (d) for **P1**, (e) for **P2**, and (f) for **P3**, respectively.

dx.doi.org/10.1021/ma300640n | *Macromolecules* 2012, 45, 4540−4549

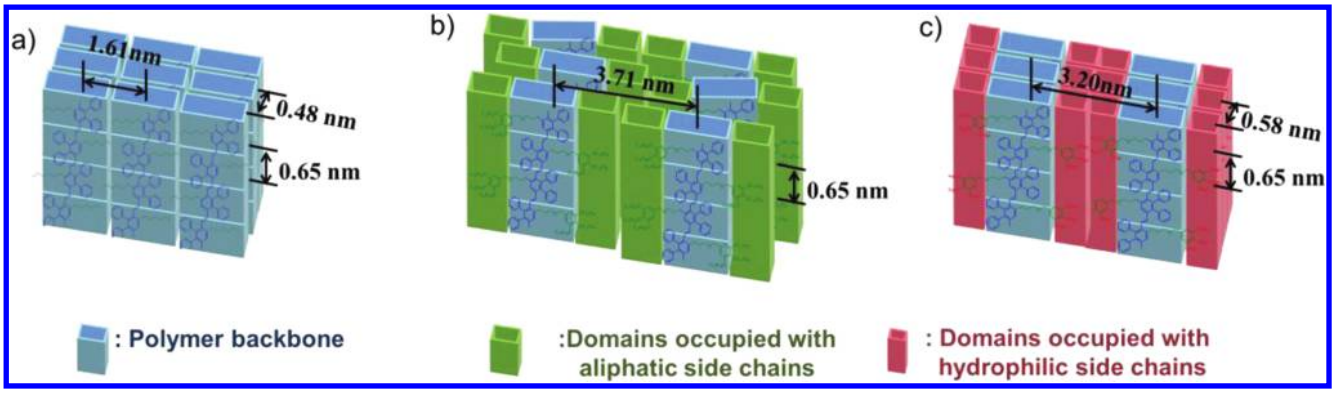

Figure 6. Schematic illustration of the phase structures of the ordered phases of (a) **P1**, (b) **P2**, and (c) **P3**. The conjugated polymer backbone is represented as a blue board, the domain occupied with the aliphatic side chains of **P2** is represented as a green board, and the hydrophilic domain occupied with the oligo(ethylene oxide) chains of **P3** is represented as a red board.

of **P2** are identical, and the thermal treatment led to an increase in the overall fraction and average domain sizes of the ordered domain in the sample of **P2**.

A combination of the DSC and 1D WAXD results provides the information regarding the structure evolution of **P1**−**P3**. To study the detailed supramolecular structures and packing symmetry, 2D WAXD of **P1**−**P3** were measured. Figure 5 shows the 2D WAXD patterns and corresponding molecular dimensions of **P1**−**P3**. The samples were sheared at temperatures slight higher than the T_is of the respective polymers and then cooled to room temperature to be used in the following 2D WAXD measurements. Along the meridian direction, a diffraction arc with *d*-spacing of 0.65 nm (2θ = 13.61°) was observed for all three polymers. Since **P1**−**P3** share the same DP-PPV structure on their conjugated backbones, and the length of a DP-PPV repeat unit is 0.65 nm along the chain direction as shown in Figure 5d−f, the diffraction arc corresponds to the periodic arrangement of the DP-PPV units along the polymer chain direction. It is also confirmed that, in the sheared samples of **P1**−**P3**, the polymer chains are aligned with the shear direction. The diffraction arcs on the equator can thus be used to identify the ordered structures along the lateral direction of the polymer chain. In Figure 5a, multiple diffraction arcs were observed along the equator and in the quadrant for ordered phase of **P1**, while in Figure 5, parts b and c, diffraction arcs were only observed on the equator for the ordered phase of **P2** and **P3**. The results confirm the ordered phase of **P1** as a crystalline phase, and those of **P2** and **P3** as liquid crystalline mesophases. For **P2**, the single diffraction arc along the equator may indicate a lamellar structure with quasi-long-range order along the lateral direction of the conjugate backbone. As for **P3**, in Figure 5c, a set of three diffractions arcs were observed on the equator located at 2θ = 2.76° (*d*-spacing: 3.20 nm), 2θ = 8.32° (*d*-spacing: 1.06 nm), and 2θ = 14.05° (*d*-spacing: 0.63 nm). These three diffractions have scattering vector (q) ratio of 1:3:5, which is an indication of the presence of a long-range ordered lamellar structure with its lamellar normal perpendicular to the chain axis. Notably, at the high 2θ angle region on the equator, a strong diffraction arc located at 2θ = 18.4° corresponding to a *d*-spacing of 0.48 nm was observed in **P1** (Figure 5a), and a weak diffraction arc located at 2θ = 17.4° corresponding to *d*-spacing of 0.51 nm was observed in **P3** (Figure 5c), while only amorphous hole was observed in this region in **P2** (Figure 5b). The *d*-spacings fall into the distance of periodic π−π stack of conjugate molecules. Thus, the extend of intermolecular π−π interaction in the ordered phases of **P1** and **P3** could be higher than it is in the ordered phase of **P2**.

The lateral packings of **P1**−**P3** were further investigated by the comparison between the lateral dimensions and the equatorial diffractions of **P1**−**P3**. For each polymer, the diffraction arc at the lowest 2θ angle on the equator represents the largest *d*-spacing of the periodic structure on the lateral direction. In Figure 5a−c, such diffraction peaks are located at 2θ = 5.48° (*d*-spacing: 1.61 nm) for **P1**, 2θ = 2.38° (*d*-spacing: 3.71 nm) for **P2**, and 2θ = 2.76° (*d*-spacing: 3.20 nm) for **P3**. As shown in Figure 5d, the lateral dimension of **P1** is 1.68 nm, which matches well with observed *d*-spacing of 1.61 nm. The significantly larger lateral *d*-spacings observed in **P2** (3.71 nm) and **P3** (3.20 nm) clearly indicate that the much bulkier dendritic side chains of **P2** and **P3** increase the lateral interchain distance tremendously. Most importantly, for **P2**, the lateral interchain distance of 3.71 nm is much smaller than the lateral dimension of **P2** (5.60 nm) with its dendritic side chains fully extended. Therefore, instead of extending, the aliphatic side chains of **P2** have to fold and the domain occupied with the aliphatic side chains is amorphous as confirmed by the amorphous halo centered at 19.61° shown in Figure 4b. The randomness in the domain occupied with the dendritic alkyl chains disturbs the stacking of the conjugated backbones, and results in a quasi-long-range ordered lamellar structure. Thus, although P2 molecules have preferable chain orientation, their conjugated backbones are not well stacked, which decreases the degree of intermolecular π−π interactions. Such phase structure explains the lack of the diffraction arc in the high angle region of **P2** (Figure 5b). On the other hand, the hydrophilic dendrons of **P3** are not as effective in hindering intermolecular π−π stacking as the hydrophobic dendrons of **P2** do. It may be due to the hydrophilic dendrons tend to further segregate from the hydrophobic conjugated polymer backbones. The segregation enhanced the lateral order and resulted in the long-range ordered lateral lamellar structure of **P3**, but made the hydrophilic dendrons less effective in blocking the π−π stacking of conjugated chains. A periodicity of *d*-spacing of 5.1 nm is therefore observed in the ordered phase of **P3**. The detailed structural determination of the ordered phases of the polymers is further investigated and will be published elsewhere.

On the basis of the 2D WAXD analysis, proposed molecular packings in the ordered phases of **P1**−**P3** are illustrated in Figure 6. Along the chain direction, the periodic repetition of the DP-PPV units separated with spacing of 0.65 nm can be

dx.doi.org/10.1021/ma300640n | *Macromolecules* 2012, 45, 4540−4549

seen in the ordered phases of **P1**−**P3**. The lateral interchain distance is 1.61 nm for **P1**, 3.71 nm for **P2**, and 3.20 nm for **P3**, which increases as the bulkiness of the pendant groups increase. Periodic arrangement along the $\pi-\pi$ stacking direction can be observed in the ordered phases of **P1** (Figure 6a) and **P3** (Figure 6c), but it is absent in the ordered phase of **P2** (Figure 6b) due to the bulkiness and random arrangement of the aliphatic dendritic pendants of **P2**. Thus, the intermolecular $\pi-\pi$ interactions of **P2** are strongly disturbed. Most importantly, such effect remains even when the ordering of the solid-state structure takes places, and may explain why the photophysical properties of **P2**, such as Φ_{PL} and PL relaxation time are much less sensitive to its solid-state phase structure.

The correlation between the Φ_{PL} and phase structure of **P1**−**P3** can be found when we compare the phase structures of **P1**−**P3** and their Φ_{PL} shown in Table 2. The Φ_{PL}s of the as-casted **P1**−**P3** films are 0.65, 0.77, and 0.63. After the thermal treatment, the Φ_{PL}s of the **P1**−**P3** films became 0.33, 0.71, and 0.38. On the basis of the previous studies, the less ordered structure of conjugated polymers used in PLED normally results in a less extend of intermolecular $\pi-\pi$ interactions and thus, higher Φ_{PL}.[34] On the contrary to that, **P2**, which possesses the most ordered structure among the three dried samples, shows the highest Φ_{PL} in the as-casted thin films of **P1**−**P3**. In addition, the structural ordering induced by the thermal treatment led to a significant decrease in the Φ_{PL} of **P1** and **P3**, but showed only negligible effect on Φ_{PL} of **P2**. This phenomenon indicates the ordering of DP-PPV molecules does not necessarily leads to a decrease in Φ_{PL}, as long as it does not involve a significant increase in the extend of intermolecular $\pi-\pi$ interactions. The effective hindering of the intermolecular $\pi-\pi$ interactions by the dendritic side chains in **P2** allows the preservation of Φ_{PL} in the environment with ordered packing of DP-PPV molecules.

CONCLUSIONS

In summary, novel DP-PPV polymers bearing hydrophobic Percec-type dendrons (**P2**) and hydrophilic Percec-type dendrons (**P3**) as side chains were successfully synthesized via Gilch route. Along with the well-known highly emissive **P1**, their structure−photophysical property relations were investigated. High Φ_{PL}s were measured for the solutions (>80%) and the as-casted films (>63%) of **P1**−**P3**. Drastic decrease of the Φ_{PL} of **P1** and **P3** were observed when the ordering of solid-state structure takes place, while **P2** still preserves its high Φ_{PL} even after the formation of its ordered mesophase. The longest PL lifetime of **P2** among the three polymers also indicates that excitons of **P2** are confined more effectively for emissive relaxation. Structural analysis by the WAXD experiments shows the periodic $\pi-\pi$ stacking is absent in the ordered phase of **P2**, but can be observed in those of **P1** and **P3**. Thus, it can be concluded that the aliphatic Percec-type dendrons of **P2** effectively disturbed the intermolecular $\pi-\pi$ interactions of the conjugated DP-PPV backbones even when structural ordering in the solid phase occurs, which effectively confines the excitons for radiative emission and alleviates the self-quenching effect. These unique properties give **P2** the potential to provide efficient and highly thermal stable luminescence in the optoelectronic applications.

ASSOCIATED CONTENT

Supporting Information

^{1}H spectra, TGA thermograms and WAXD patterns of the *I* phases. This material is available free of charge via the Internet at http://pubs.acs.org.

AUTHOR INFORMATION

Corresponding Author

*Telephone: +886-3513-1523. Fax: +886-3513-1523. E-mail: (C.-L.W.) kclwang@nctu.edu.tw; (C.-S.H.)cshsu@mail.nctu.edu.tw.

Notes

The authors declare no competing financial interest.

ACKNOWLEDGMENTS

The authors thank the National Science Council and the "ATP Program" of the Ministry of Education, Taiwan, for financial support.

REFERENCES

(1) Burroughes, J. H.; Bradley, D. D. C.; Brown, A. R.; Marks, R. N.; Mackay, K.; Friend, R. H.; Burns, P. L.; Holmes, A. B. *Nature* **1990**, *347*, 539−541.
(2) Braun, D.; Heeger, A. J. *Appl. Phys. Lett.* **1991**, *58*, 1982−1984.
(3) Yang, S.-H.; Hsu, C.-S. *J. Polym. Sci., Part A: Polym. Chem.* **2009**, *47*, 2713−2733.
(4) Bao, Z.; Lovinger, A. J. *Chem. Mater.* **1999**, *11*, 2607−2612.
(5) Cheng., Y.-J.; Yang, S.-H.; Hsu, C.-S. *Chem. Rev.* **2009**, *109*, 5868−5923.
(6) Akcelrud, L. *Prog. Polym. Sci.* **2003**, *28*, 875−962.
(7) Jenekhe, S. A.; Osaheni, J. A. *Science* **1994**, *265*, 765−768.
(8) Rothberg, L. J.; Yan, M.; Papadimitrakopoulos, F.; Galvin, M. E.; Kwock, E. W.; Miller, T. M. *Synth. Met.* **1996**, *80*, 41−58.
(9) Ahn, T.; Jang, M. S.; Shim, H.-K.; Hwang, D.-H.; Zyung, T. *Macromolecules* **1999**, *32*, 3279−3285.
(10) Pang, Y.; Li, J.; Hu, B.; Karasz, F. E. *Macromolecules* **1999**, *32*, 3946−3950.
(11) Liao, L.; Pang, Y.; Ding, L.; Karasz, F. E.; Smith, P. R.; Meador, M. A. *J. Polym. Sci., Part A: Polym. Chem.* **2004**, *42*, 5853−5862.
(12) Cyriac, A.; Amrutha, S. R.; Jayakannan, M. *J. Polym. Sci., Part A: Polym. Chem.* **2008**, *46*, 3241−3256.
(13) Lee, J.-I.; Kang, I.-N.; Hwang, D.-H.; Shim, H.-K.; Jeoung, S. C.; Kim, D. *Chem. Mater.* **1996**, *8*, 1925−1929.
(14) Alam, M. M.; Jenekhe, S. A. *Macromol. Rapid Commun.* **2006**, *27*, 2053−2059.
(15) Ahn, T.; Ko, S.-W.; Lee, J.; Shim, H.-K. *Macromolecules* **2002**, *35*, 3495−3505.
(16) Jeong, H. Y.; Lee, Y. K.; Talaie, A.; Kim, K. M.; Kwon, Y. D.; Jang, Y. R.; Yoo, K. H.; Choo, D. J.; Jang, J. *Thin Solid Films* **2002**, *417*, 171−174.
(17) Lee, N. H. S.; Chen, Z.-K.; Huang, W.; Xu, Y.-S.; Cao, Y. *J. Polym. Sci., Part A: Polym. Chem.* **2004**, *42*, 1647−1657.
(18) Xiao, S.; Nguyen, M.; Gong, X.; Cao, Y.; Wu, H.; Moses, D.; Heeger, A. J. *Adv. Funct. Mater.* **2003**, *13*, 25−29.
(19) Resmi, R.; Amrutha, S. R.; Jayakannan, M. *J. Polym. Sci., Part A: Polym. Chem.* **2009**, *47*, 2631−2646.
(20) Wu, C.-W.; Tsai, C.-M.; Lin, H.-C. *Macromolecules* **2006**, *39*, 4298−4305.
(21) Peng, Q.; Xu, J.; Li, M.; Zheng, W. *Macromolecules* **2009**, *42*, 5478−5485.
(22) Hsieh, B. R.; Yu, Y.; Forsythe, E. W.; Schaaf, G. M.; Feld, W. A. *J. Am. Chem. Soc.* **1998**, *120*, 231−232.
(23) Hsieh, B. R.; Wan, W. C.; Yu, Y.; Gao, Y.; Goodwin, T. E.; Gonzalez, S. A.; Feld, W. A. *Macromolecules* **1998**, *31*, 631−636.
(24) Yang, S.-H.; Chen, J.-T.; Li, A.-K.; Huang, C.-H.; Chen, K.-B.; Hsieh, B.-R.; Hsu, C.-S. *Thin Solid Films* **2005**, *477*, 73−80.

(25) Yang, S.-H.; Li, H.-C.; Chen, C.-K.; Hsu, C.-S. *J. Polym. Sci., Part A: Polym. Chem.* **2006**, *44*, 6738−6749.
(26) Yang, S.-H.; Chen, S.-Y.; Wu, Y.-C.; Hsu, C.-S. *J. Polym. Sci., Part A: Polym. Chem.* **2007**, *45*, 3440−3450.
(27) Liao, Y.-M.; Shih, H.-M.; Hsu, K.-H.; Hsu, C.-S.; Chao, Y.-C.; Lin, S.-C.; Chen, C.-Y.; Meng, H.-F. *Polymer* **2011**, *52*, 3717−3724.
(28) Percec, V.; Bera, T. K.; Glodde, M.; Fu, Q.; Balagurusamy, V. S. K.; Heiney, P. A. *Chem.—Eur. J.* **2003**, *9*, 921−935.
(29) Rosen, B. M.; Wilson, C. J.; Wilson, D. A.; Peterca, M.; Imam, M. R.; Percec, V. *Chem. Rev.* **2009**, *109*, 6275−6540.
(30) Kimura, M.; Sato, M.; Adachi, N.; Fukawa, T.; Kanbe, E.; Shirai, H. *Chem. Mater.* **2007**, *19*, 2809−2815.
(31) Bao, Z.; Amundson, K. R.; Lovinger, A. J. *Macromolecules* **1998**, *31*, 8647−8649.
(32) Jakubiak, R.; Bao, Z.; Rothberg, L. *Synth. Met.* **2000**, *114*, 61−64.
(33) Marsitzky, D.; Vestberg, R.; Blainey, P.; Tang, B. T.; Hawker, C. J.; Carter, K. R. *J. Am. Chem. Soc.* **2001**, *123*, 6965−6972.
(34) Chou, C.-H.; Shu, C.-F. *Macromolecules* **2002**, *35*, 9673−9677.
(35) Balagurusamy, V. S. K.; Ungar, G.; Percec, V.; Johansson, G. *J. Am. Chem. Soc.* **1997**, *119*, 1539−1555.
(36) Li, W.; Zhang, A.; Feldman, K.; Walde, P.; Schlüter, A. D. *Macromolecules* **2008**, *41*, 3659−3667.
(37) Sun, R. G.; Wang, Y. Z.; Wang, D. K.; Zheng, Q. B.; Kyllo, E. M.; Gustafson, T. L.; Epstein, A. J. *Appl. Phys. Lett.* **2000**, *76*, 634−636.
(38) Sohn, B.-H.; Kim, K.; Choi, D. S.; Kim, Y. K.; Jeoung, S. C.; Jin, J.-I. *Macromolecules* **2002**, *35*, 2876−2881.
(39) Lo, K.-H.; Ho, R.-M.; Liao, Y.-M.; Hsu, C.-S.; Massuyeau, F.; Zhao, Y.-C.; Lefrant, S.; Duvail, J.-L. *Adv. Funct. Mater.* **2011**, *21*, 2729−2736.
(40) Cullity, B. D., *Elements of X-Ray Diffraction*: Addison-Wesley: Reading, MA, 1956.